**Atmospheric
Chemistry
and Physics**

Aerosol and thermodynamic effects on tropical cloud systems during TWPICE and ACTIVE

P. T. May[1], G. Allen[2], G. Vaughan[2], and P. Connolly[2]

[1]Centre for Australian Weather and Climate Research – A partnership between the Bureau of Meteorology and CSIRO, Australia
[2]University of Manchester, UK

Abstract. Regularly occurring storms over the Tiwi Islands, north of Darwin, Australia are used as a laboratory for investigating the relative importance of thermodynamic parameters, shear and aerosols on the amount and intensity of convection over the islands during the pre-monsoon and monsoon break periods of the 2005–2006 summer wet season. Storm systems on individual days are characterised by simple metrics derived from polarimetric radar data. The analysis shows clear dependencies on thermodynamic and shear parameters. The shear dependence was unexpected, as high shear implied less activity, but this is likely an island effect. There are some indications of a dependence of storm intensity on aerosol, but mid-level moisture differences may also play a role.

1 Introduction and background

There has been considerable debate in the scientific community concerning the potential impacts of aerosols on convective clouds. This has come about from a number of modelling and observational studies of such clouds that indicate that aerosol concentrations have a profound impact on storm intensity and lifetime (e.g. Rosenfeld and Lensky, 1998; Khain et al., 2005; Koren et al., 2005; van den Heever et al., 2006; Cotton et al., 2007). However, there is great uncertainty regarding the magnitude of these effects compared with other

factors such as the boundary layer thermal and shear structure. Many of the studies to examine these influences have been based on models. Observations to test these ideas are difficult, because of the substantial variations in the thermodynamic structure and forcing at different locations in addition to aerosol variations. This makes it difficult to isolate the relative mechanisms and quantify their influence.

However, the Darwin area in Northern Australia may offer an opportunity to test some of these ideas observationally with relatively clear separation of competing effects. In the build and break periods of the Australian monsoon there are strong locally forced thunderstorms that form over the Tiwi Islands, about 80 km north of Darwin, on ∼80% of days (Keenan et al., 1989, 2000). These deep convective storms are known colloquially as "Hector" and have been the subject of numerous observational and modelling studies, at least partly because of its relative predictability (e.g., Keenan et al., 1989, 2000; Carey and Rutledge, 2000; Golding, 1993; Simpson et al., 1993; Carbone et al., 2001; Wilson et al., 2001; Crook, 2001; Saito et al., 2001, Vaughan et al., 2008).

The forcing for these storms is relatively constant; being due to sea-breeze convergence coupled with an otherwise relatively weak low-level mean flow, and constant sea surface temperature. Furthermore, the Tiwi islands are sufficiently small such that the low-level winds replace the island boundary layer every night so that a new island boundary layer growth starts afresh in the morning (Schafer et al., 2001). Thus the gross boundary layer structure on the island has relatively uniform characteristics from day to day, although the

CAPE, CIN[1] and shear do vary with changing synoptic conditions. The islands are large enough that successive interactions between storm outflows and the sea breeze allows a multi-stage convective development with large numbers of cumulus mergers (e.g. Carbone et al., 2001; Simpson et al., 1993). These storms form in a wide variety of CAPE, shear and aerosol environments (e.g. Keenan and Carbone, 1992; Allen et al., 2008). The local thermodynamics can be estimated/paramaterised using routine WMO soundings from nearby Darwin airport (150 km to the south).

There is a strong seasonal dependence of aerosol characteristics in northern Australia (Allen et al., 2008; Luhar et al., 2008). Early in the build up of the wet season, prior to the monsoon onset (typically November/December), the atmosphere is relatively smoky due to widespread biomass burning as a result of routine annual land management in the nearby Arnhem Land area to the east of Darwin (e.g. Mitchell, 2002: http://www.eoc.csiro.au/agsnet/tropas.htm). As the build up continues throughout December these fires typically decrease, but the low-level continental flow ensures that aerosol concentrations remain reasonably high (see Allen et al., 2008, for further details). This build up is followed by active monsoon periods, with a prevalent pristine maritime flow and wide-scale oceanic convection. However, the aerosol loading during breaks in the monsoon, when thermodynamic and convective properties return to monsoon build up conditions, remains very low due to the cessation of the biomass burning source.

This contrast in local aerosol loading, whilst dynamic forcing properties remain relatively constant in the build up and monsoon break periods, allows an investigation of whether or not significant variations in observed storm characteristics may depend on aerosol regimes. This requires that such signals must first be separable from other factors such as thermodynamic controls. There were a number of major field campaigns undertaken in the Darwin area during the Austral summer of 2005 and 2006 (described by Vaughan et al., 2008; and May et al., 2008), which provide data to address this issue. These campaigns included detailed in situ aircraft aerosol and chemistry measurements in the Darwin area as well as radar operations (see following section). Data collected during these campaigns have been analysed here to examine these questions.

2 Data

Three sources of data are used in this analysis: Aircraft measurements of aerosol content and chemistry, radiosonde soundings from Darwin Airport and gridded radar reflectivity and microphysical classification data generated from a research polarimetric radar (C-Pol, described by Keenan et al., 1998). The aircraft measurements used here were recorded by the UK Natural Environment Research Council (NERC) Dornier-228 up to an operational ceiling of 4 km. The aircraft was deployed on science flights to circumnavigate the Tiwi Islands to provide thermodynamic and composition profiles of the local boundary layer before and during convective inflow to Hector storms. The aircraft was equipped with thermodynamic sensors, fine and coarse-mode aerosol sizing spectrometers, an aerosol mass spectrometer measuring submicron non-refractory aerosol composition; as well as gas phase instruments measuring a range of VOCs, CFCs, carbon monoxide and ozone. For further details of the Dornier aircraft configuration, instrumentation and data quality, see Allen et al. (2008).

The 09:00 a.m. (Local time) sounding data are analysed routinely by the Australian Bureau of Meteorology operational forecasters and estimates of the Convective Available Potential Energy (CAPE) and Convective Inhibition (CIN) are produced from the soundings for both inland and coastal locations. This estimate is made using a so-called modified sounding where forecasters adjust surface parcel characteristics to allow for heating and moistening from surface fluxes and the consequent growth in, and mixing of, the BL and related entrainment processes. This procedure is widely employed around the world. This study used the operational estimate of coastal CAPE as this is expected to be most appropriate for the Tiwi Islands.

While the above observations define the environment, radar is an ideal tool to describe convective systems. The C-Pol radar is a 5.5 cm wavelength scanning polarimetric weather radar system presently located at Gunn Point (12.25° S, 131.04° E) near Darwin (see Keenan et al., 1998 for further details). The radar provides measurements of the reflectivity (Z_H), differential reflectivity (Z_{DR}), absolute differential phase on propagation (Φ_{DP}) as well as its derivative in range, the Specific Differential Phase (K_{DP}); and finally the correlation of the signals at the two polarisations ($\rho_{HV}(0)$). These parameters and their use are discussed in many papers (e.g. Keenan et al., 1998; Zrnic and Ryzhkov, 1999). A polarimetric radar has at least two significant capabilities compared with conventional radar. Firstly it is possible to measure rainfall much more accurately than using

---

[1] The Convective available potential energy of a parcel is defined as

$$\text{CAPE} = \int_{\text{LFC}}^{\text{LNB}} g \frac{\theta c - \theta \text{env}}{\theta \text{env}} dz$$

where θc is the virtual potential temperature of a parcel and θenv is the environmental virtual potential temperature, g is the acceleration due to gravity, LFC is the level of free convection and LNB is the level of neutral buoyancy. Convective inhibition, CIN is defined similarly

$$\text{CIN} = \int_{\text{zl}}^{\text{LFC}} g \frac{\theta c - \theta \text{env}}{\theta \text{env}} dz$$

except the integration limits are between the origin height of the parcel (here a surface parcel) and the LFC.

reflectivity alone. This is because rainfall estimators can be optimised for different rainfall rates including using information of the underlying drop size distributions and correct for the effects of radar attenuation. The second major capability is the determination of hydrometeor species. Different hydrometeors occupy different parts of the $[Z_H, Z_{DR}, K_{DP}, \rho_{HV}(0),$ temperature] phase space so the combination of the above parameters can be used with good success to estimate the dominant hydrometeors in a particular cloud location (e.g. May and Keenan, 2005).

3 Analysis methods

In order to examine the storm characteristics statistically, metrics for the storm characteristics are required. Detailed individual analysis of large numbers of individual cases is both difficult and not the ideal method to obtain quantitative measures for comparing the storms in different regimes. However, a methodology for characterising convection in a volume of radar data with some simple metrics has been developed by May and Lane (2008). First, a three-dimensional cloud mask can be formed based on gridded radar reflectivity data. Then we seek to obtain height-resolved statistics from these gridded data. A simple approach is to calculate the fraction of a domain that is covered by radar echoes greater than some nominal reflectivity value as well as the fractional coverage of rain, snow etc and the height profile of the maximum reflectivity within the domain as a function of time and height. Thus the approach is as follows:

1. Interpolate the radar reflectivity and microphysical classifications from the polarimetric radar data onto a Cartesian grid.

2. For a domain covering the Tiwi Islands (Fig 1) calculate at each altitude level of the grid:

    a. The fraction of the area covered by $Z>[10, 20, 30, 40]$ dBZ

    b. The fraction of the area covered by rain, snow, graupel, hail

    c. The maximum reflectivity anywhere in the grid

With these data for each Hector case, a simple metric to describe the overall system is simply to take the largest value of the areas and maximum reflectivity at any time or height within individual storm systems. The underlying distributions for the rain, and 10 dBZ areas as well as the maximum height of the 40 dBZ are Gaussian. However, not all the 40 dBZ areas pass a Gaussian test when sorted for low CIN, high shear or by CAPE with the distributions showing some skewness. However, the results are similar if medians rather than means are used but the absolute significance values of the 40 dBZ area differences using t tests should be treated with some caution.
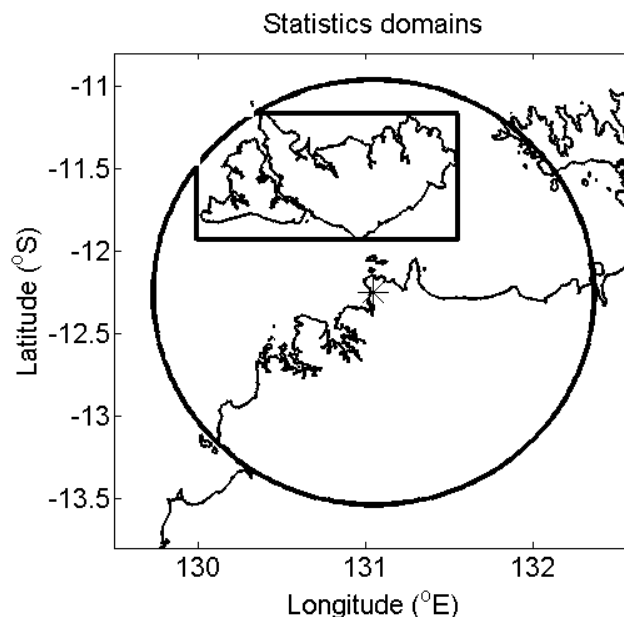

Fig. 1. Tiwi Island domain for the collection the radar statistics. The circle marks the radar volume coverage and the star is the radar location. The statistics are the fraction of the domain covered by reflectivity greater than [0, 10, 20, 30, 40 50] dBZ, covered by rain, snow, graupel, and hail as well as the maximum reflectivity in the domain as a function of height and time.

These derived data sets can then be augmented. For example it is convenient to calculate the area total rainfall, as well as the convective and stratiform contributions, to the average rain and the relative areas and mean rain rates of the convective and stratiform rain. The convective and stratiform components here are separated using the algorithm described by Steiner et al. (1995).

Not all the metrics described give useful proxies for all cases. For example, the maximum height of the 20 and 30 dBZ echoes have often been used as proxies for storm intensity, but it turns out that at some time in almost all the Hector cases examined the 30 dBZ contour reaches the tropopause. Thus the maximum height of these reflectivity contours is not a useful discriminant of system intensity. The height of the 40 dBZ contour seems a much more useful proxy for storm intensity as this varies by significant amounts. There are also several parameters that are highly correlated, e.g. the maximum area of snow and 10 dBZ are quite similar. This is not surprising since the reflectivity and temperature are prime inputs into the microphysical classification (Keenan, 2003).

4 Characterisation of data sets

The C-Pol radar began operation for the 2005/2006 wet season on 10 November 2005 and continued well into March
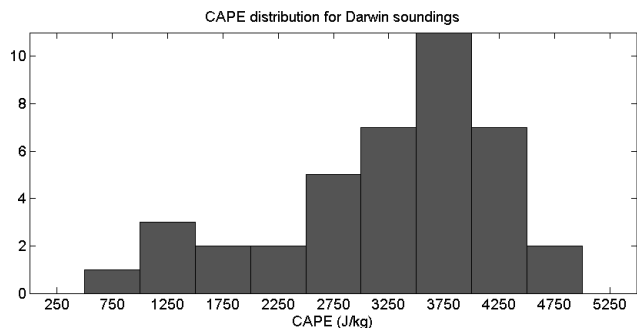
Fig. 2. Distribution of CAPE estimated from operational Darwin soundings for the Hector days.

Fig. 3. Scatter plot of the Darwin CAPE and magnitude of the zonal wind shear between 200 and 2500 m for the days used in this analysis. Points are colour coded for high (red) and low (blue) aerosol days.

Table 1. Means of the boundary layer aerosol concentrations measured in #/cc observed with the Dornier.

Period	Fine Mode (21–4.5 μm)	Coarse mode (1.6–32 μm)
10 November–13 December 2005	72±23	0.08±0.04
6–14 February 2006	42±14	0.17±0.14

2006. The characteristic easterly jet associated with build up conditions (Drosdowsky, 1996) was present through December 2005 except for a brief episode of surface and mid-level westerlies (Vaughan et al., 2008) and an extended break in the monsoon was observed beginning on 5 February and extending to 28 February 2006 (May et al., 2008). During these easterly jet phases there were 44 Hector cases observed, with 12 of these coincident with flight operations. Days when there was no clearly definable Hector storm, or where the situation was complicated by squall lines or overnight and early morning convection, were excluded from this analysis. A time window of 0:00–12:00 UTC (09:30–21:30 local) is used for the radar, but the peaks in radar coverage have not been observed before 02:00 UTC.

A histogram of the analysed CAPE values for these 44 cases is shown in Fig. 2. The CAPE for these modified soundings tends to be high, but there is a clear peak in the distribution at about 3700 J/kg with a tail extending down to values less than about 2500 J/kg. Thus for our sorting of high versus low CAPES we use a criterion of greater (less) than 2500 J/kg for high (low) CAPE cases. There are more high CAPE cases, but there remain a reasonable number of low CAPE examples and these are evenly distributed through the analysis period. A similar analysis can be done for CIN (not shown). Here the operational values are often extremely low and the selected threshold between low and high CIN is 8 J/kg. This low threshold ensures a reasonably similar number of low and high CIN cases, but similar results are obtained for somewhat higher threshold values of CIN. Note also that there is a reasonably high negative correlation ($\sim$−0.6) between high CAPE and low CIN in the data set.

A third control may be the vertical shear of the horizontal wind. This has been shown to be important in a range of observational, theoretical and modelling studies (e.g., Rotunno et al., 1988; LeMone et al., 1998; Moncrieff and Liu, 1999). The general result of these studies has been that high shear favours increasing intensity of convection. This is complicated for the analysis here by the climatological jet profile with an easterly maximum near 700 hPa that is present (Ke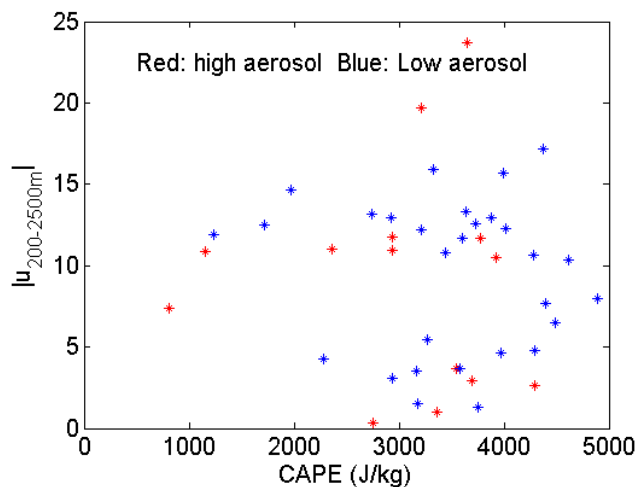enan and Carbone, 1992). However, based on the the-oretical arguments of the above studies, low level shear is expected to show some impact on storm intensities. The data have been sorted by the shear between the near surface and the approximate climatological jet maximum. A good approximation for this is the 200 m to 2500 m shear. Both total and the zonal component of the shear have been examined. Here the data will be stratified into two levels, low ($|u_z| < 8\,\text{ms}^{-1}$), and high ($|u_z| > 8\,\text{ms}^{-1}$), shear. These thresholds give similar sample sizes for each criterion.

Sub-cloud aerosol data collected by the Dornier aircraft sorted by the prevailing meteorological conditions (see Allen et al., 2008) can be used to characterise two aerosol regimes: the period prior to Christmas 2005 can be classified as a period of relatively high fine-mode aerosol ($D < 4.5\,\mu$m) concentrations; and relatively low concentrations during the February break period. The aerosols were characterised by organics and black carbon in the early part of the pre-Christmas period with organics making an increasing fraction as time went on. Fine mode aerosol in the February data consist mainly of organics, but there was an increase in coarse mode aerosol in the latter period, albeit still with low absolute concentrations (Table 1).
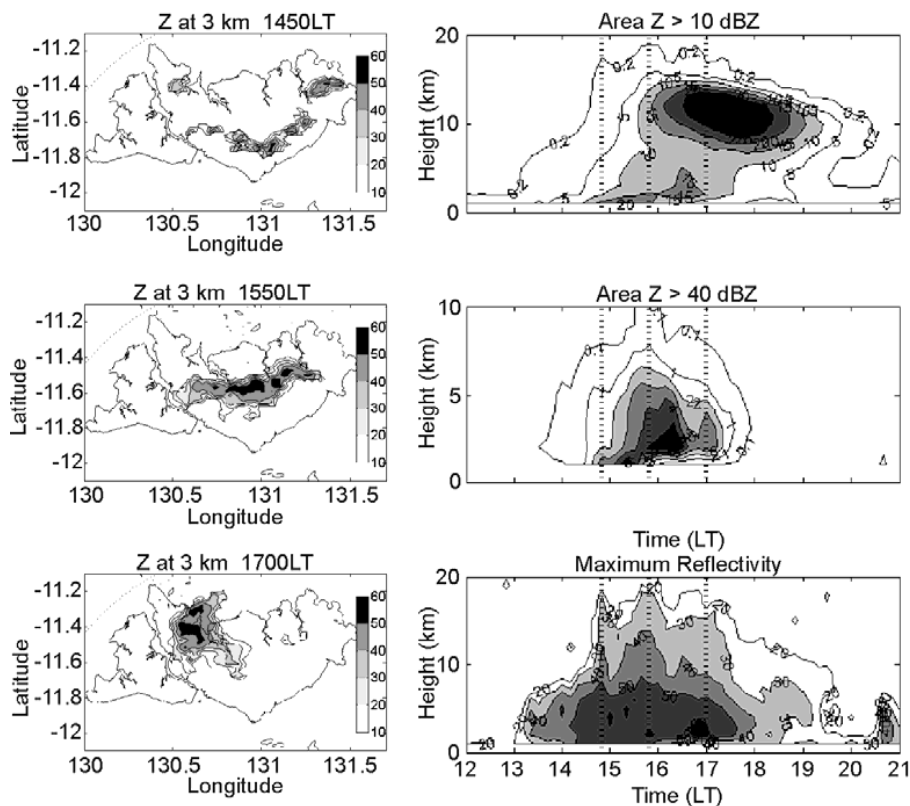
Fig. 4. A series of three constant altitude plots of radar reflectivity over the Tiwi Islands (left) and corresponding Statistical Coverage Products of the 10 and 40 dBZ areas along with a time-height cross-section of the maximum reflectivity anywhere in the island domain for 10 February 2006. The vertical dashed lines mark the times of the radar images.

These aircraft observations were supported by observations of aerosol optical depth (AOD) taken using a CIMEL sun photometer to the east and inland at the CSIRO Jabiru observing site where the mean AOD at visible wavelengths was approximately 0.18–0.20 in the early period and 0.12–0.15 in the latter period. This is important as there are many Hector cases used in this analysis that were seen after the aircraft operations ceased. Another important consideration is that the mean and standard deviations of the CAPE, CIN and shear values are almost identical for the two aerosol regimes. Figure 3 shows a scatter plot of the shear against CAPE in Darwin with colour coding for the high and low aerosol regimes. This shows the independence of the shear, CAPE and aerosol content and some separation of the shear regimes. It is desirable to sort the data such that there is a clear separation of regime for example by only analysing the top and bottom quartiles, but with the small data set this is difficult and with the small data sample the significance of the results to follow does not vary much.

5   An example of "Hector": 10 February 2006

As noted above, the storms over the Tiwi Islands are extremely regular. The initial convection on the island typically occurs on the peninsulas where there is local convergence on sea breezes, and on the sea breeze front that opposes the low level flow (Wilson et al., 2001). There is a heat low over the Australian continent at these times of year with a layer of surface westerlies a few hundred metres deep. These have the effect of steepening the sea breeze front on the eastern end of the islands and this is where the initial storms form (e.g. Wilson et al., 2001; Fig. 4). These initial storms do not usually reach great intensity, but the outflow from them interact with the sea breeze farther along the coast. Furthermore, mergers of cells begins to occur with significant enhancements of storm intensity (Simpson et al., 1993). This stage is seen in Fig. 4b where the convection is concentrated into a few strong cells and this is when the 40 dBZ contour reached the greatest height indicating that the strongest updrafts were at this time. These interactions between storms outflows and sea breezes continue until the outflows dominate and there is a realignment of the storms as the shear and outflows dominate (Keenan et al., 1989; Carbone et al., 2001; Fig. 4c). It is during this process that the maximum area of reflectivities
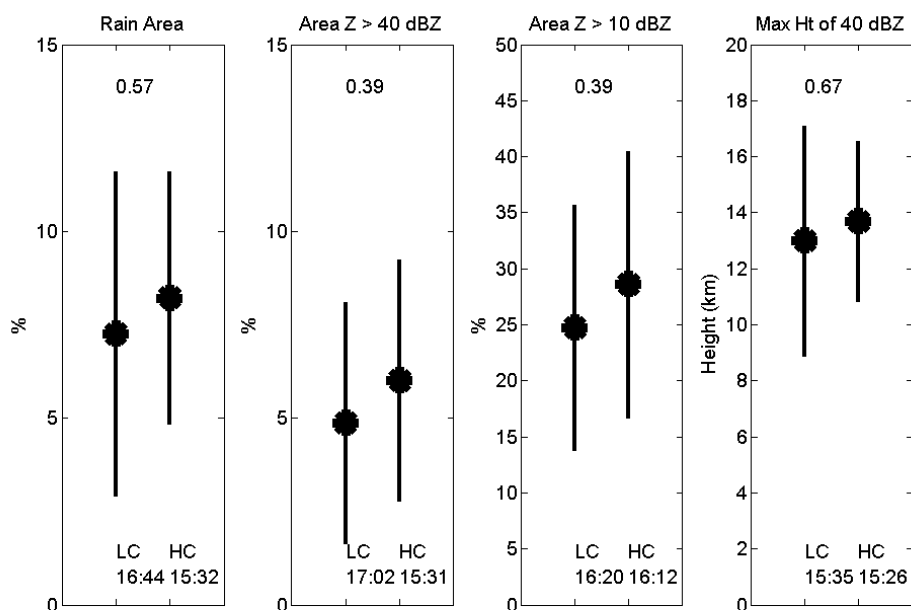
Fig. 5. Mean and standard deviation of the maximum area covered by rain, the time of that maximum, maximum area covered by 40 dBZ, the maximum area covered by 10 dBZ, and the maximum height of the 40 dBZ echo for a given day. The data are stratified by the operational estimate of CAPE from Darwin soundings into high (HC:CAPE>2500 J/kg) and low CAPE (LC) samples. The mean local time of these maxima is given below the labels and the probability that the two samples have equal means is given at the top of the figure.

>40 dBZ are reached. The anvil production is also peaking at this time as can be seen in the area of reflectivity >10 dBZ maximising around the time of the last radar image.

The example of the Hector in Fig. 4 is typical of the afternoon storms over the islands. As noted above, a sample of 44 such cases have been analysed here and there are examples of both weaker and stronger storms scattered through the season. The analysis and comparisons discussed here will focus on the maximum areas of rain, 10 dBZ and 40 dBZ echoes, as well as the height of the 40 dBZ echo contour. As discussed in the previous section, the latter three parameters are proxies for anvil area, convective area and maximum updraft intensity.

6 Results

The analysis in this section will show the means and standard deviations of the maximum values of the indicators describing individual cases calculated for samples of several storms. Figure 5 shows the mean and standard deviation of the maximum values discussed when the Hector cases are sorted by CAPE. The mean areas and maximum height of the 40 dBZ echoes and their standard deviations are plotted. The mean time that the various maxima occur is also given along with the probability that the means are the same based on a T-test with the sampled variances. There are some factors that need to be remembered when interpreting these results. Firstly CAPE is very sensitive to errors in the low level parcel char-

acteristics and humidity in particular (e.g. Weckwerth, 2000). This is complicated by the use of manually modified soundings as discussed above. Thus individual CAPE values have large uncertainties due to meteorological noise that is difficult to quantify, such that a significant amount of smearing across cases with a real signal may be expected. There are also relatively few low CAPE cases. Nevertheless there is a clear consistent signal seen, with the high CAPE cases on average producing larger areas of rain, convection, and anvil and more intense cells, albeit with a considerable spread in the data. The actual buoyancy profile may also affect the storms as well as absolute values of CAPE, and some indication of this will be discussed later for data sorted by the aerosol regimes. The individual differences are not significant at the 95% level, but taken together with individual significance levels ∼0.6 (1-Pr (means are the same)) show a clear trend. Furthermore, all these maxima occur earlier in the day in the high CAPE sample compared with the low CAPE cases. These results are also supported by the maximum area averaged rainrates and total accumulation that were significant at a modest (∼0.7) level.

Figure 6 describes the results of a similar analysis with the data sorted by CIN as discussed in Sect. 4. Despite the anti-correlation with CAPE, there are significant differences in the way the data stratifies and the statistical significance of the differences. The low CIN cases produce larger areas of rain (sig∼0.96) and anvil (sig∼0.7) as may be expected with smaller inhibition for storm initiation. However, in contrast to the CAPE results, the high CIN cases on average produce
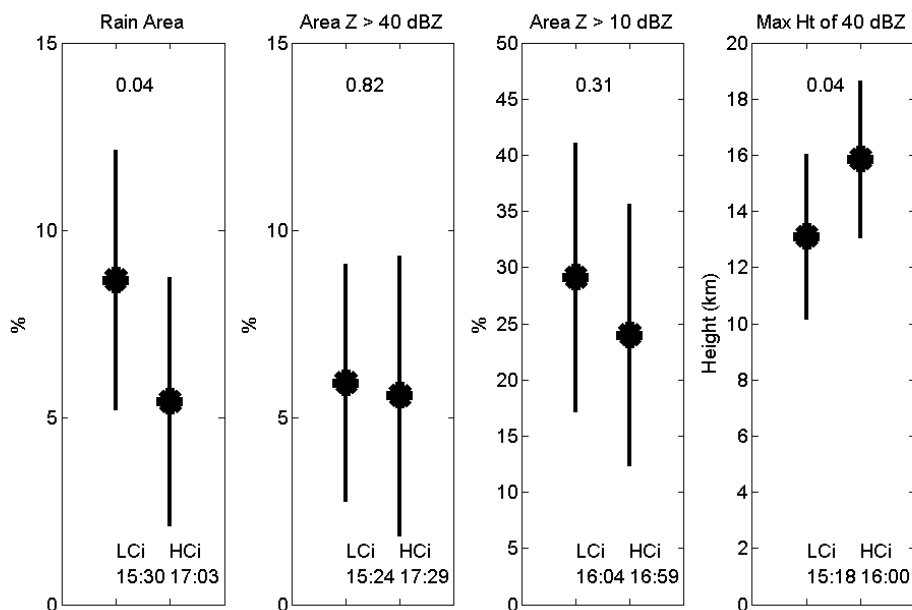
Fig. 6. As for Fig. 5, except the data are stratified by CIN with low CIN (LCi) classed as <12 J/kg and high CIN (HCi>12 J/kg).

more intense cells at some stage of the storm system lifecycle (sig∼0.96) while the maximum convective area was essentially independent. This is consistent with the idea that when the inhibition is high, deep convection is delayed and the potential energy of the boundary layer can grow to larger values before it is released. Furthermore, stronger forcing may be required to initiate the convection and both these factors will tend to more intense storms. The maximum area of convection was only slightly higher for the low CIN cases, but high values of CIN substantially delayed the occurrence of this maximum. That is, there was more time required to heat the boundary layer to produce this convection. This likely limited the time available for anvil production through several cycles of new initiation, mergers and reorganisation of the storm (Carbone et al., 1999) and less production of anvil cloud. However, these differences did not translate into significant differences in area averaged maximum rainrate or accumulated rain.

The last of the thermal and dynamical constraints to be examined is the vertical wind shear. The results of this analysis are shown in Fig. 7 and clearly show a trend toward decreasing storm activity and intensity with increasing shear with high statistical significance. These differences map onto the rain statistics with the high shear regime producing substantially less rain than the low shear with significance at ∼0.97. This is somewhat surprising as most observational studies in open ocean or continental regions, as well as modelling and theoretical calculations, point to increasing potential for storm intensity with increasing shear (e.g. Moncrieff and Liu, 1999) although the picture is more complex for shears greater than those accounted for here (e.g. Weisman and Klemp, 1982). Shear can also affect the organisation of lines (e.g.

LeMone et al., 1998) but in the Hector cases predominantly accounts for a re-organisation of sea-breeze oriented convection into shear perpendicular squall line configurations in the mature storm system phase (Keenan et al., 2000). However, the current case is on a relatively small island and the shear correlates with the wind speed itself. Thus the residence time of boundary layer air over the island is reduced for the increasing winds, decreasing the time available for boundary layer growth and CAPE development on such islands. Furthermore, the storm systems themselves will be advected off the islands more quickly reducing the scope for mergers and consequent increase in convective area and storm intensity.

This now leads to testing the idea that aerosol characteristics may act as a primary control of convective characteristics. Figure 8 shows the mean and standard deviation of the maximum areas and other metrics for Hector cases sorted by aerosol regime. There is very little difference evident in the means of the 40 dBZ areas, the anvil areas (10 dBZ), and several other parameters not shown such as the maximum reflectivity and hail area across the two aerosol regimes. However, there are two parameters that do show significant differences. The height of the 40 dBZ echoes, which is a proxy for updraft strength, is on average lower in the clean regime. The other significant difference appears as a greater maximum rain area in the cleaner environment. The greater area also results in higher accumulated rainfall over the islands, but importantly, the maximum area averaged total and convective rainrates were actually higher in the low aerosol regime (at a sig∼0.85) in contrast to the weaker intensity of individual cells. The rain maximum occurs slightly later in the day in the clean cases and after the convective maximum, but before the maximum in anvil area is observed. The similarity
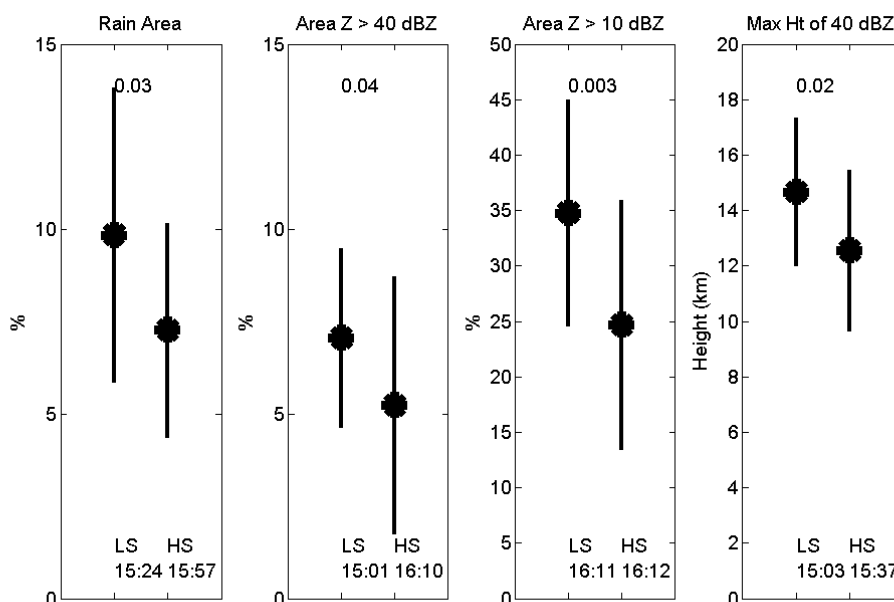
Fig. 7. As for Fig. 5, except we have two classes of wind shear between 200 and 2500 m. These are for zonal shear $<8\,\mathrm{ms}^{-1}$ (LS) and shear$>8\,\mathrm{ms}^{-1}$ (HS). Again the times of the mean are given below the labels and the probabilities of equal means are given.
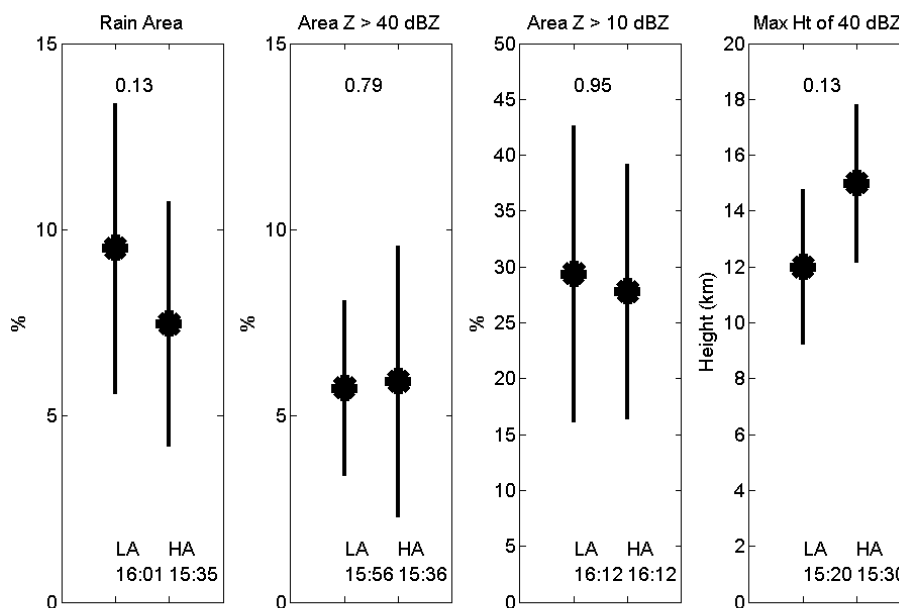

Fig. 8. As for Fig. 5, but with two categories for high (HA), and low aerosols (LA) sorted by date with LA being February and March 2006 and HA being November and December 2005 cases.

of the maximum 40 dBZ area and the time lag implies that the enhanced rain area is associated with stratiform rain.

The question of whether such differences are a direct consequence of the different aerosol regimes remains. It seems that the observed rain area is an unlikely candidate as the anvil areas were generally similar. One mechanism for a larger stratiform rain area compared with anvil area is if the

mid-levels were significantly more moist, reducing evaporation of the settling ice particles. Analysis of the profiles of the equivalent potential temperature as measured by Darwin radiosondes for the analysis period (Fig. 9) show that on average the mid-level moisture is higher during the break (low aerosol) than in the build up periods, although still much less than during the monsoon while the corresponding potential
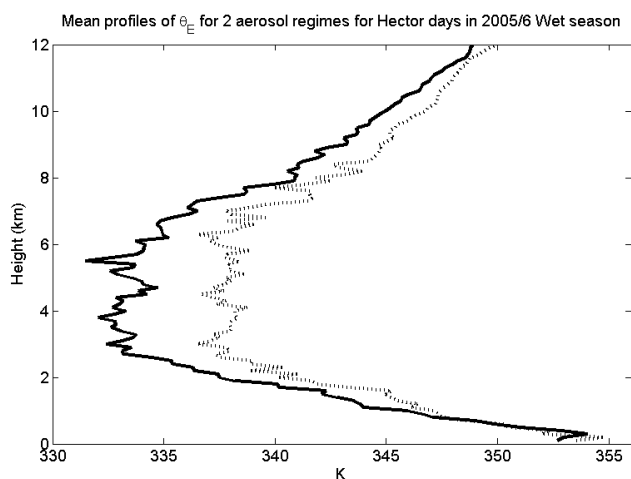
Fig. 9. Profiles of the mean equivalent potential temperature profile for Hector days in the high aerosol (solid) and low aerosol (dashed) regimes.

temperature profiles were almost identical (not shown). This difference may affect the dynamics. Drier mid-levels may enhance downdraft strength through more efficient evaporation of rain droplets which in turn provide stronger forcing for new updrafts, so the picture is somewhat complicated. However, the aerosol may also affect the rate of cloud particle nucleation which in turn may affect the updraft strength through changes in the balance between warm rain and ice dominated processes (e.g. Khain et al., 2005; van den Heever et al., 2006). It is interesting to note that another proxy for updraught strength, particularly near the freezing level is the hail area and this was uniform for all cases. Hail occurrence is sensitive to the updraft strength at the freezing level while the height of the 40 dBZ echo is an indication of deeper updraft strength. Thus, although the height of the 40 dBZ echo is a proxy for the maximum updraft strength, it seems to be occurring well above the freezing level.

7 Conclusions

This study has examined the statistics of thunderstorms that occurred over the Tiwi Islands during the Australian monsoon build up and break phases of the 2005/2006 wet season (November to February). The results of a statistical analysis of Hector characteristics with the data sorted by thermodynamic controls such as CAPE and CIN show considerable spread, but the means clearly correspond to expected results that high CAPE leads to more extensive and intense convection albeit with relatively low levels of statistical significance. High CIN tends to produce smaller areas of convection, but the individual storms are more intense. This is clearly consistent with ideas regarding thermodynamic controls on convective activity.

A goal of the analysis was to try and isolate aerosol controls separately from variations in the thermodynamics. This was only partially successful. There was a clear progression of aerosol loadings during the experimental period that lent itself to this analysis and the mean thermodynamic parameters were almost identical across the aerosol regimes. Several of the average storm characteristics were hardly affected by the environmental changes associated with the different aerosol loading regimes. The exceptions to this were the maximum height of the 40 dBZ echo and rain area. The rain area was most likely associated with systematic variations in mid-level moisture, but the storm intensity is more complex with both aerosol and thermodynamic effects are potentially implicated. There is a need for detailed cloud-resolved modelling (CRM) work to resolve this issue. These results are somewhat different to those of Koren et al. (2005) and others who found that high aerosols tended to be associated with greater anvil cover as well as more intense convection in satellite diagnoses of Atlantic storms. Further work is needed to extend this work to examine if there are systematic variations in rain drop size distributions in cloud systems in the different thermodynamic and aerosol regimes. These can be performed using polarimetric radar retrievals of rain median volume diameters (e.g. Brandes et al., 2004; Williams and May, 2008)

References

Allan, J. D., Jimenez, J. L., Williams, P. I., Alfarra, M. E., Bower, K. N, Jayne, J. T., Coe, H., and Worsnop, D. R.: Quantitative sampling using an Aerodyne Mass Spectrometer 1, Techniques of data interpretation and error analysis, J. Geophys. Res. Atmos., 108, 4090–4099, 2003.

Allan, J. D., Coe H., Bower, K., N., Alfarra, M. R., Delia, A. E., Jimenez, J. L., Middlebrook, A. M., Drewnick, F., Onasch, T. B., Canagaratna, M. R., Jayne, J. T., and Worsnop, D. R.: A generalised method for the extraction of chemically resolved mass spectra from Aerodyne aerosol mass spectrometer data, J. Aerosol. Sci., 35, 909–922, 2004.

Allen, G., Vaughan, G., et al.: Aerosol and trace-gas measurements in the Darwin area during the wet season, J. Geophys. Res., 113, D06306, doi:10.1029/2007JD008706, 2008.

Ben Liley, J., Baumgardner, D., Kondo, Y., Kita, K., Blake, D. R., Koike, M., Machida, T., Takegawa, N., Kawakami, S., Shirai

T., and Ogawa, T.: Black carbon in aerosol during BIBLE B, J. Geophys. Res., 108, 8399, doi:10.1029/2001JD000845, 2003.

Brandes, E. A., Zhang, G., and Vivekanandan, J.: Drop size distribution retrieval with polarimetric radar, model and application, J. Appl. Meteor., 43, 461–475, 2004.

Carbone, R. E., Wilson, J. W., Keenan, T. D., and Hacker, J. M.: Tropical island convection in the absence of significant topography Part I, Life cycle of diurnally forced convection, Mon. Weather Rev., 128, 3459–3480, 2000.

Carey, L. D. and Rutledge, S. A.: The relationship between precipitation and lightning in tropical island convection, A C-band polarimetric radar study, Mon. Weather Rev., 128, 2687–2710, 2000.

Cotton, W. R., Zhang, H., McFarquhar, G. M., and Saleeby, S. M: Should we consider polluting Hurricanes to reduce their intensity?, J. Wea. Modif., 39, 70–73, 2007.

Crook, N. A.: Understanding Hector, The dynamics of island thunderstorms, Mon. Weather Rev., 129, 1550–1563, 2001.

Drosdowsky, W.: Variability of the Australian summer monsoon at Darwin, 1957–1992, J. Clim., 9, 85–96, 1996.

Golding, B. W.: A numerical investigation of tropical island thunderstorms, Mon. Weather Rev., 121, 1417–1433, 2003.

Jimenez, J. L., Jayne, J. T., Shi Q., et al.: Ambient aerosol sampling using the Aerodyne Mass Spectrometer, J. Geophys. Res., 108, 8425–8437, 2003.

Keenan, T. D.: Hydrometeor classification with a C-band polarimetric radar, Aust. Meteor. Mag., 52, 23–31, 2003.

Keenan, T. D. and Carbone, R. E.: A preliminary morphology of precipitation systems in tropical northern Australia, Quart. J. Roy. Meteor. Soc., 118, 283–326, 1992.

Keenan, T. D., Morton, B. R., Manton, M. J., and Holland, G. J.: The Island Thunderstorm Experiment (ITEX) – A study of tropical thunderstorms in the Maritime Continent, Bull. Amer. Meteor. Soc., 70, 152–159, 1989.

Keenan, T. D., Glasson, K., Cummings, F., Bird, T. S., Keeler, J. and Lutz, J.: The BMRC/NCAR C-Band polarimetric (C-POL) radar system., J. Atmos. Oceanic Tech., 15, 871–886, 1998.

Keenan, T. D., Rutledge, S. A., et al.: The Maritime Continent Thunderstorm Experiment (MCTEX), Overview and some results, Bull. Amer. Meteor. Soc., 81, 2433–2455, 2000.

Khain, A., Rosenfeld, D., and Pokrovsky, A.: Aerosol impact on the dynamics and microphysics of deep convective clouds, Quart. J. Roy. Meteor. Soc., 131, 2639–2663, doi:10.1256/qj.04.62, 2005

Koren, I., Kaufman, Y. J., Rosenfeld, D., Remer, L., and Rudich, Y.: Aerosol invigoration and restructuring of Atlantic convective clouds, Geophys. Res. Lett., 32, L14828, doi:10.1029/2005GL023187, 2005.

LeMone, M. A., Zipser, E. J., and Trier, S. B.: The role of environmental shear and thermodynamic conditions in determining the structure and evolution of mesoscale convective systems during TOGA COARE, J. Atmos. Sci, 55, 3493–3518, 1998.

Luhar, A. K., Mitchell, R. M., Meyer, C.H., Campbell, S. K., and Gras, J. L.: Biomass burning emissions over Northern Australia constrained by aerosol measurements II – Model validation and impacts on air quality and climate, Atmos. Environ., 42, 1647–1664, 2008.

May, P. T. and Keenan, T. D.: Evaluation of microphysical retrievals from polarimetric radar with wind profiler data, J. Appl. Meteor., 44, 827–838, 2005.

May, P. T. and Lane, T. P.: A method for using weather radar data to test cloud resolving models, Met. Appl., submitted, 2008.

May, P. T., Mather, J. H., Vaughan, G., Jakob, C., McFarquhar, G. M., Bower, K. N., and Mace, G. G.: The Tropical Warm Pool International Cloud Experiment (TWPICE), Bull. Amer. Meteor. Soc., 89, 629–645, 2008.

Moncrieff, M. W. and Liu, C.: Convection initiation by density currents, Role of convergence, shear, and dynamical organization, Mon. Weather Rev., 121, 2455–2464, 1999.

Rosenfeld, D. and Lensky, I. M.: Satellite-based insights into precipitation formation processes in continental and maritime convective clouds, Bull. Amer. Meteor. Soc., 79, 2457–2476, 1998.

Rotunno, R., Klemp, J. B., and Wiseman, M. L.: A theory for strong long-lived squall lines, J. Atmos. Sci., 45, 463–485, 1998.

Saito, K., Keenan, T. D., Holland, G., and Puri, K.: Numerical simulation of the diurnal evolution of tropical island convection over the maritime continent, Mon. Weather Rev., 129, 378–400, 2001.

Schafer, R., May, P. T., Keenan, T. D., McGuffie, K., Ecklund, W. L., Johnson, P. J., and Gage, K. S.: Island boundary layer development over a tropical island during the Maritime Continent Thunderstorm Experiment (MCTEX), J. Atmos. Sci., 58, 2163–2179, 2001.

Simpson, J., Keenan, T. D., Ferrier, B., Simpson, R. H., and Holland, G. J.: Cumulus mergers in the maritime continent, Meteor. Atmos. Phys., 51, 73–99, 1993.

Steiner, M., Houze, R. A. Jr, and Yuter, S. E.: Climatological characterization of three-dimensional storm structure from operational radar and rain gauge data, J. Appl. Meteor., 34, 1978–2007, 1995.

Straka, J. M., Zrnic, D., and Ryzhkov, A.: Bulk hydrometeor classification and quantification using polarimetric radar data, Synthesis of relations, J. Appl. Meteor., 39, 1341–1372, 2000.

Vaughan, G., Schiller, C., MacKenzie, A. R., Bower, K., Peter, T., Schlager, H., Harris, N. R. P., and May, P. T.: Studies in a natural laboratory, High-altitude aircraft measurements around deep tropical convection, Bull. Amer. Meteor. Soc., 89, 647–662, 2008.

Van Den Heever, S. C., Carrio, G. G., Cotton, W. R., deMott, P. J. and, Prenni, A. J.: Impacts of nucleating aerosol on Florida storms Part I, Mesoscale simulations, J. Atmos. Sci, 63, 1752–1775, 2006.

Weckwerth, T. M.: The effect of small-scale moisture variability on thunderstorm initiation, Mon. Weather Rev., 128, 4017–4030, 2000.

Weisman, M. L. and Klemp, J. B.: The dependence of numerically simulated convective storms on vertical wind shear and buoyance, Mon. Weather Rev., 110, 504–520, 1982.

Williams, C. R. and May, P. T.: Uncertainties in Profiler and Polarimetric DSD Estimates and their Relation to Rainfall Uncertainties, J. Atmos. Oceanic Tech., 25, 1881–1887, 2008.

Wilson, J. W., Carbone, R. E., Tuttle, J. D., and Keenan, T. D.: Tropical island convection in the absence of significant topography Part II: Nowcasting storm evolution, Mon. Weather Rev., 129, 1637–1655, 2001.

Zrnic, D. S. and Ryzhkov, A.: Polarimetry for weather surveillance radars, Bull. Amer. Meteor. Soc., 80, 389–406, 1999.